

Dielectric Resonator-Based Flow and Stopped-Flow EPR with Rapid Field Scanning: A Methodology for Increasing Kinetic Information

Andrzej Sienkiewicz,*† Ana Maria da Costa Ferreira,‡ Birgit Danner,†§ and Charles P. Scholes^{¶,1}

**Institute of Physics, Al. Lotnikow 32, 02-668, Warsaw, Poland;* ‡*Instituto de Química, Universidade de São Paulo, 05508 São Paulo, Brazil;*

§*Department of Physics, Würzburg University, Am Hubland, 57074 Würzburg, Germany;* and †*Physics Department and*

¶*Chemistry Department, State University of New York at Albany, Albany, New York 12222*

Received November 3, 1997; revised July 21, 1998

We report methodology which combines recently developed dielectric resonator-based, rapid-mix, stopped-flow EPR (appropriate for small, aqueous, lossy samples) with rapid scanning of the external (Zeeman) magnetic field where the scanning is pre-programmed to occur at selected times after the start of flow. This methodology gave spectroscopic information complementary to that obtained by stopped-flow EPR at single fields, and with low reactant usage, it yielded more graphic insight into the time evolution of radical and spin-labeled species. We first used the ascorbyl radical as a test system where rapid scans triggered after flow was stopped provided “snapshots” of simultaneously evolving and interacting radical species. We monitored ascorbyl radical populations either as brought on by biologically damaging peroxynitrite oxidant or as chemically and kinetically interacting with a spectroscopically overlapping nitroxide radical. In a different biophysical application, where a spin-label lineshape reflected rapidly changing molecular dynamics of folding spin-labeled protein, rapid scan spectra were taken during flow with different flow rates and correspondingly different times after the mixing-induced inception of protein folding. This flow/rapid scan method is a means for monitoring early immobilization of the spin probe in the course of the folding process.

© 1999 Academic Press

Key Words: rapid scan stopped-flow EPR.

INTRODUCTION

Rapid, homogeneous mixing of two reactants then followed by flow or stopped-flow methods is a primary technique to determine the mechanism and rate of chemical reactions. When paramagnetic species form, decay, or change, rapid-mix flow and stopped-flow methods combined with EPR provide direct kinetic measurement of their chemistry. Technical details of a newly developed, nonstandard stopped-flow system based on a small high sensitivity dielectric resonator (DR) were described in Ref. (1). This structure, having a nearby rapid mixer and fluid flow system with low dead volume, was then applied to follow the kinetic folding/unfolding of spin-labeled yeast iso-

1-cytochrome *c* (2). The kinetic behavior was conventionally monitored at one field position in the EPR spectrum. With optical spectroscopy, considerably more kinetic information is known to be accessed with a rapid wavelength scan of entire spectra. Similarly, with EPR spectroscopy considerably more kinetic information on paramagnetic species that interact, evolve, and spectroscopically overlap can be accessed with rapid field scanning. After flow was stopped, rapid-field-scanned EPR traces, where the time scale for scanning was considerably less than the time scale of the kinetics, showed overall kinetic behavior for radical build-up and decay. Since the DR has high sensitivity and freedom from flow and stopped-flow artifacts (1, 3), rapid field scanned spectra were obtained with good signal-to-noise and low reactant usage during flow. With such rapid scan during flow we observed species that have evolved only for a time equal to the dead time of the apparatus.

EXPERIMENTAL

Technical description. The dielectric resonator-based stopped-flow system has been previously reported (1). A general scheme of our stopped-flow EPR system with modification for rapid scan is shown in the block diagram of Fig. 1. The Model 715 syringe ram controller from Update Instrument, Inc. (Madison, WI), provided a synchronizing start pulse for the syringe drive ram and provided programmable flow rates and flow times. When we were monitoring EPR amplitude at a single magnetic field, such a pulse would also directly trigger the data collection system operating with Scientific Software Services Systems (Bloomington, IL) EW 2.41A software. When a rapid field scan occurring at a definite time after start of flow was additionally to be used, the synchronizing pulse from the syringe drive controller triggered a delay circuit which in turn triggered the rapid scan unit field sweep. The source of the triggerable rapid scan field sweep was the Bruker rapid scan unit (Bruker ER-420). The field sweeping ramp from the rapid scan unit was routed to a home-built rapid scan amplifier and thence to fast sweep coils positioned in the air

¹ To whom correspondence should be addressed. Fax: 518-442-3462. E-mail: cps14@cnsvox.albany.edu.

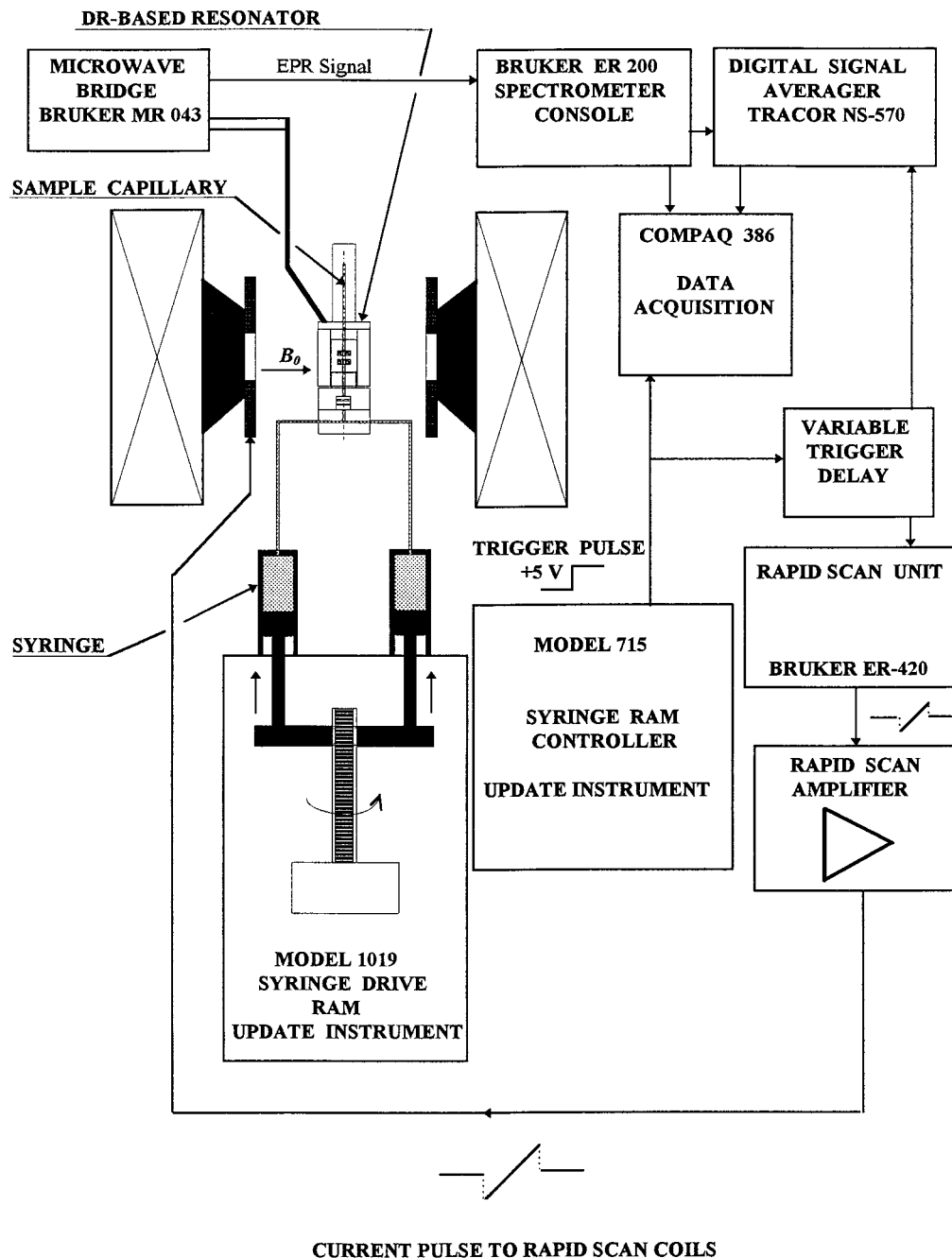


FIG. 1. Block diagram of the stopped-flow EPR system modified for triggered, synchronized rapid field scan and for subsequent rapid scan data collection.

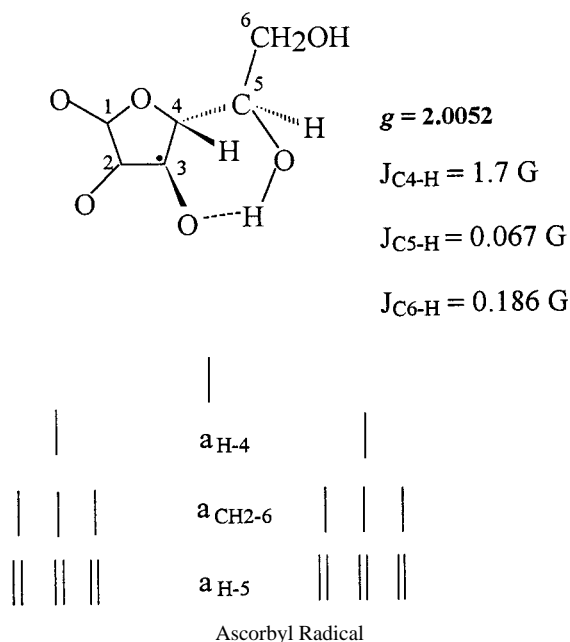
gap of the electromagnet. The rapid scan amplifier was previously developed for pulse field-sweep EPR (4, 5), a cryogenic hole-burning EPR technique, unrelated to these ambient temperature kinetic studies. We found it useful for minimal ramp distortion to connect the fast sweep coils to the power amplifier by a shielded twisted pair cable instead of a regular coaxial cable. With this field sweep unit we generated a linear field sweep up to 60 G in width over a period of 0.1 s. (Narrower field sweeps could be generated

over a shorter time.) Spectra from rapid field sweeps were collected by a Tracor 570 signal averager and subsequently stored in a PC computer that was equipped with an IBM DAC card. Dead times were estimated from the known flow rate and 8- μ L dead volume between the mixer and center of the resonator and confirmed experimentally from the rapid destruction of the spin probe TEMPOL (4-hydroxy-2,2,6,6-tetramethyl-1-piperidinyloxy) by sodium dithionite reductant.

Materials. Peroxynitrite was prepared from sodium nitrite and hydrogen peroxide in a quenched flow reactor, as previously described (6) with minor modifications; excess hydrogen peroxide was removed by treatment with granular MnO_2 . The final solution was kept frozen at -78°C , from which peroxynitrite solutions were prepared to the desired concentration by dilution in 0.1 M NaOH and analyzed by absorbance at 302 nm ($\epsilon = 1670 \text{ M}^{-1} \text{ cm}^{-1}$) (7). All the solutions were prepared using glass-distilled water and reagents. The buffer solutions used in the experiments with peroxynitrite were also pretreated with Chelex-100 as a precaution against transition metal ion contamination. L-Ascorbic acid and TEMPOL (Sigma) were dissolved in the suitable buffers at the desired concentrations. Yeast iso-1-cytochrome *c* spin-labeled at the naturally occurring cysteine¹⁰² sulfur with the cysteine-specific spin-label methanethiosulfonate (MTSSL) spin-label was prepared as in Ref. (2).

RESULTS AND DISCUSSION

Rapid scan applied to build-up and decay of radicals. Ascorbic acid (Vitamin C) can lead to time-evolving radical systems either directly in the form of the ascorbyl radical itself ($\text{Asc}^{\cdot-}$) or indirectly by causing reduction and decay of other radicals. The EPR signal of the ascorbyl radical signal presents considerable hyperfine detail whose resolution represents a practical test of EPR signal-to-noise, especially when carried out with rapid scan and a small instrumental time constant. The structure of the oxygen-centered ascorbyl radical is shown in Scheme 1. It has a two-line EPR signal centered at $g = 2.0052$ due to its large 1.7 G coupling with the C4 proton and couplings to C5 and C6 protons that are an order of magnitude smaller than 1.7 G (8).



SCHEME 1

Ascorbate itself can act as a reductant for other observable radicals, notably the common spin probe TEMPOL. The TEMPOL signal is a three-line signal with splitting of $\sim 17.2 \text{ G}$ that reflects the hyperfine interaction with the $I = 1 \text{ }^{14}\text{N}$ of the nitroxyl group. The presence of $\text{Asc}^{\cdot-}$ causes destruction of the TEMPOL, and the $\text{Asc}^{\cdot-}$ and TEMPOL signals spectroscopically overlap but decay at different rates. The presence of the ascorbate causes loss of the TEMPOL signal, and the presence of the TEMPOL increases the rate of $\text{Asc}^{\cdot-}$ decay as well. When $\text{Asc}^{\cdot-}$ is present, its features overlap the central feature of TEMPOL. The feasibility of recording whole EPR spectra on a time scale that is shorter than the overall kinetics was demonstrated using $\text{Asc}^{\cdot-}$ and TEMPOL. The field-swept spectra in Fig. 2, triggered at different times after the start of flow and each lasting 100 ms, graphically show the behavior of simultaneously evolving TEMPOL and $\text{Asc}^{\cdot-}$ species. The first spectrum 2A, where $\text{Asc}^{\cdot-}$ was present in only a small amount, was taken during flow when the dead time between mixing and observation was 15 ms. $\text{Asc}^{\cdot-}$ built up to its maximum shortly after flow was stopped, as shown by Spectrum 2B initiated 25 ms after flow was stopped, and $\text{Asc}^{\cdot-}$ was still evident in Spectrum 2D initiated 925 ms after flow was stopped. The TEMPOL signal had totally disappeared within 1 s after flow was stopped. The TEMPOL/ $\text{Asc}^{\cdot-}$ system provided a simple test for the stopped flow/rapid scan procedure in resolving overlapping radical species having different, though possibly related, kinetic behavior. We note that a previous report of a stopped-flow/flow system based on a different type of small resonant structure, the loop-gap resonator developed at the National Biomedical ESR Center (9), showed a scanned spectrum of TEMPOL/ $\text{Asc}^{\cdot-}$ obtained by signal averaging during flow but not the detailed compendia of changing spectra which occurred after flow stopped.

Ascorbate is a reductant which protects against biologically damaging oxidants. Two such notable oxidants of recent interest are peroxynitrite (ONOO^-) and its acidic form, peroxynitrous acid (ONOOH) (10). Peroxynitrite is formed in cells by the reaction of nitric oxide (NO) and superoxide ($\text{O}_2^{\cdot-}$) (11). The acidic form is more reactive (12) and can be mainly responsible for the cytotoxicity attributed to peroxynitrite. The reduction of the peroxynitrite itself as brought on by ascorbate has been monitored by near-UV spectroscopy (13), and this report prepares the methodological groundwork for a comparative study of the peroxynitrite and $\text{Asc}^{\cdot-}$ kinetics. At pH 7.4 the decay time for peroxynitrous acid in the absence of ascorbate reductant itself is $\sim 1 \text{ s}$ (6). The kinetic trace of Fig. 3, obtained on the low field derivative EPR feature of $\text{Asc}^{\cdot-}$, shows the corresponding kinetic increase and decay of $\text{Asc}^{\cdot-}$ brought on by peroxynitrite oxidation. There was a rapid initial build-up of $\text{Asc}^{\cdot-}$ radical to its maximal concentration in a time of about 0.2 s after flow was stopped that was then followed by a decay of $\text{Asc}^{\cdot-}$ that stretched over $\sim 2 \text{ s}$. This latter decay was well fit to a first-order exponential and not by a second-order dismutation as has been proposed for decay of

the ascorbyl radical (14). A single 0.1-s rapid field scan trace (Inset A of Fig. 3) was acquired at the maximal $\text{Asc}^{\cdot-}$ concentration. This trace, swept over 10 G, was taken with sufficiently small modulation of 0.3 G peak-to-peak, 0.1 ms time constant, and sufficient signal-to-noise that there was evidence for structure finer than that of the largest 1.7-G splitting (8) of $\text{Asc}^{\cdot-}$. The concentration of the $\text{Asc}^{\cdot-}$ in Fig. 3, Inset A was $\sim 19 \mu\text{M}$. Inset B of Fig. 3 shows the $\text{Asc}^{\cdot-}$ signal as obtained by rapid field scan during flow and estimated at $\sim 8 \mu\text{M}$ in concentration. To produce an individual rapid scan trace on $\text{Asc}^{\cdot-}$, less than a 30- μL volume of each reactant was used.

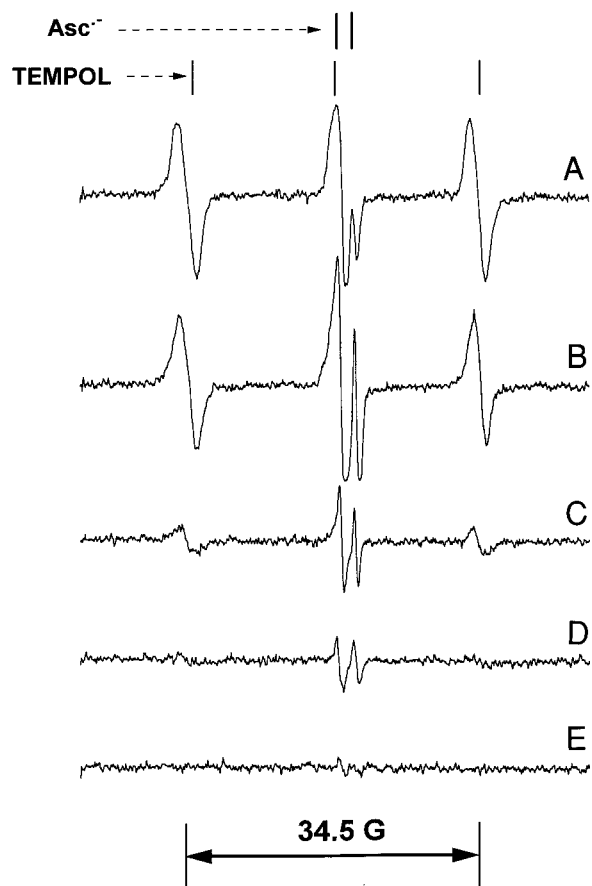


FIG. 2. This figure shows the time evolution of the partially overlapping $\text{Asc}^{\cdot-}$ and TEMPOL radicals through a compendium of rapid scan EPR spectra taken at different delays after the syringe drive and the mixing were started. Following the mixing of 400 μM TEMPOL and 0.5 M ascorbate (pH 10), the TEMPOL radical was reduced and its three-line EPR spectrum eliminated while the $\text{Asc}^{\cdot-}$ radical, occurring in the center of the spectrum, built up then decayed. Each rapid scan trace was taken with a 60-G field sweep in 0.1 s, the magnetic field modulation was 0.5 G peak-to-peak, the instrumental time constant was 0.1 ms, and each trace was from one accumulation. The microwave power was 2 mW, EPR frequency $\nu_e = 9.62$ GHz. The traces were recorded as follows: (A) during flow for which the dead time was 15 ms; (B) 25 ms after flow was stopped; (C) 625 ms after flow was stopped; (D) 925 ms after flow was stopped; and (E) 1825 ms after flow was stopped.

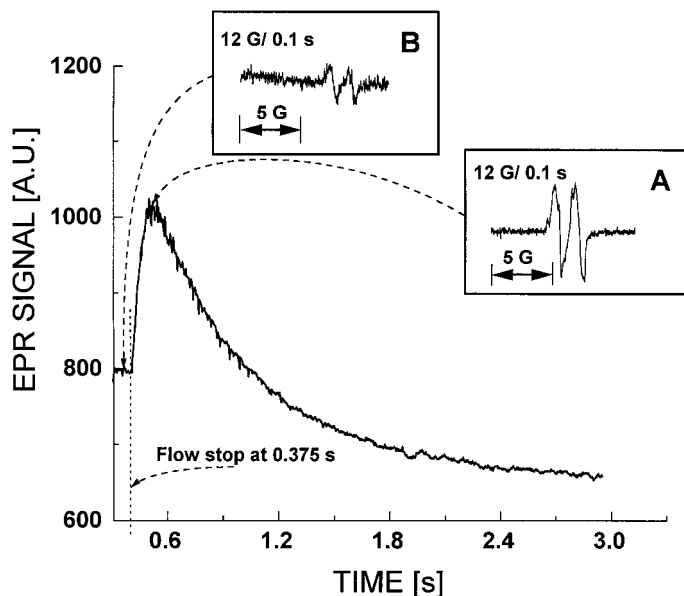


FIG. 3. The overall, single-field kinetic trace in this figure shows the time evolution of the $\text{Asc}^{\cdot-}$ signal as influenced by peroxynitrite oxidant. The single-field kinetic trace resulted from 1:1 mixing 200 mM ONOO^- with 0.5 M ascorbate at pH 9 and was taken on the low field derivative of the $\text{Asc}^{\cdot-}$ signal. Solutions were bubbled with He for ~ 5 min before each experiment, a procedure which led to deaeration and which also prevented the formation of bubbles in storage syringes. The field modulation was 0.3 G peak-to-peak, microwave power was 2 mW, EPR frequency $\nu_e = 9.62$ GHz, and the instrumental time constant for the kinetic trace taken at a single field was 1 ms. Inset (A) was from one rapid scan trace taken with a 0.1-s field sweep starting at the indicated maximal point on the kinetic trace, and Inset (B) was from one rapid scan trace taken during flow for which the dead time was 15 ms. For both of the rapid field scan insets the time constant was 0.1 ms, the field modulation was 0.3 G peak-to-peak, microwave power was 2 mW, and EPR frequency $\nu_e = 9.62$ GHz.

Rapid scan method to follow early folding of spin-labeled protein. In our folding study on yeast iso-1-cytochrome *c* spin-labeled at cysteine¹⁰², a significant fraction ($\sim 60\%$) of refolding occurred during the ~ 8 -ms dead time between mixing and subsequent observation within the DR (2). There is question in the literature whether cytochrome *c* refolding occurring in less than 20 ms is due to the formation of tertiary interactions (localized within a subdomain such as a protein C-terminal helix where our spin-label is found (15)) or due to incipient global molecular collapse (16). A goal of the flow-rapid scan method will be to document the kinetics of immobilization and to document immobilization from the lineshape of the incipiently refolding protein.

The refolding was initiated by rapid mixing and dilution of guanidinium-denatured protein with buffer. We wanted more effectively to characterize the early folding forms of our spin-labeled proteins. Such characterization is better carried out by observing the overall rapid scanned EPR spectrum during flow, where we monitor the EPR spectrum of partially refolded protein within milliseconds after refolding is initiated. We

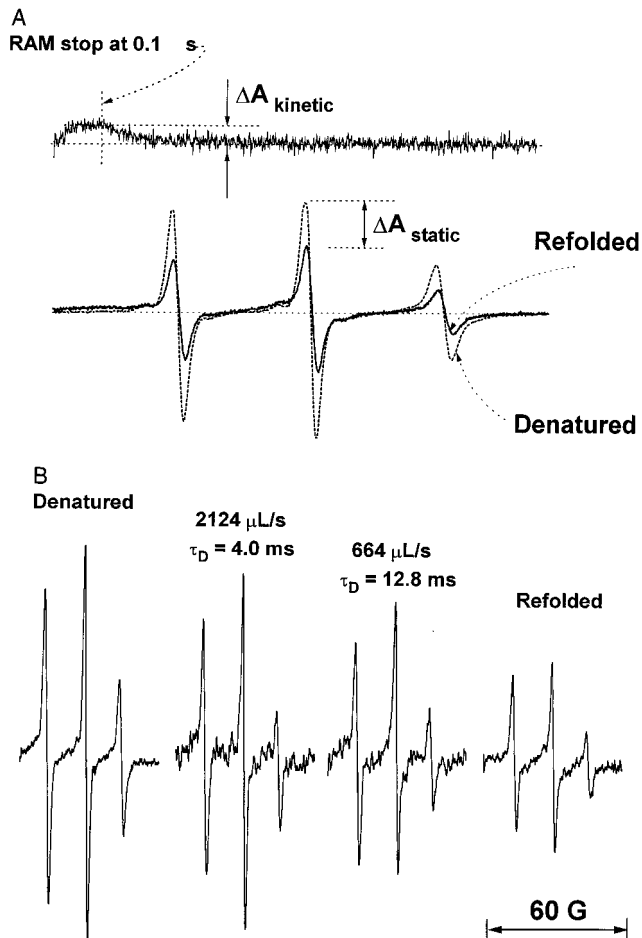


FIG. 4. (A) provides a comparison of the EPR spectra of unfolded and refolded protein taken with standard slow scans of 1-min duration. The unfolded protein was in 1.4 M guanidinium hydrochloride and 0.1 M Na acetate buffer, pH 5.0; the refolded protein was in 0.70 M guanidinium hydrochloride and 0.1 M Na acetate buffer, pH 5.0. The transient kinetic trace at a single field was taken at the central derivative extremum and was initiated by rapid mixing (dead time ~ 12.8 ms) of 0.2 mM denatured spin-labeled yeast iso-1-cytochrome *c* in 1.4 M guanidinium hydrochloride with an equal volume of 0.1 M Na acetate buffer, pH 5.0. The height of this kinetic transient was $\sim 40\%$ of the overall static difference in peak height between denatured and refolded protein. (B) shows rapid scanned EPR spectra (60 G/0.1 s) of spin-labeled protein obtained at different times after refolding was initiated. All spectra were normalized with respect to the number of scans; rapid scans were of 100-ms duration, time constant 0.5 ms, 60-G width; microwave power was 2 mW; EPR frequency $\nu_e = 9.62$ GHz. The spectra of the increasingly renatured proteins with dead times of 4.0 and 12.8 ms were each obtained with an accumulation of 4 rapid scans. The spectrum of the protein long after folding was completed and flow was stopped was obtained with 16 rapid scans. The spectrum of denatured protein was taken before mixing and is the accumulation of 16 scans; it has been multiplied by $\frac{1}{2}$ since it was not diluted by mixing. The temperature was 6.5°C.

varied the dead time of observation by varying the programmable flow rate. In Fig. 4A we first compare the slowly accumulated (not rapid scanned) spectra from protein denatured by guanidinium chloride and from refolded protein, and

we show the transient change in signal induced by stopped-flow-induced refolding as monitored at the central peak. In Fig. 4B we compare signal-averaged rapid scanned spectra (60-G rapid scans of 100 ms duration) from unfolded protein before flow started, from partially refolded protein obtained with 4.0- and 12.8-ms dead times *during flow*, and from refolded protein long after flow was stopped. The spectrum obtained at the faster flow rate and shorter 4.0-ms dead time showed sharper, more intense derivative EPR features than those of the spectrum obtained with the slower flow rate and longer 12.8-ms dead time because the protein had ~ 8 ms less time to refold and to enfold the probe subsequent to mixing. Approximately 20% of the signal change between unfolded and refolded forms had occurred within 4.0 ms, whereas $\sim 50\%$ of the signal change had occurred within 12.8 ms. The spectra with 4.0- and 12.8-ms dead times each consisted of four separate signal-averaged scans where the respective total consumptions of spin-labeled protein were 0.84 and 0.26 mL. For doing these measurements, including the multiple-scan signal averaging, the total sample usage was ~ 5 mg of protein.

ACKNOWLEDGMENTS

Acknowledgment is made to the Donors of the Petroleum Research Fund, administered by the American Chemical Society, for partial support of this research (PRF 29658-AC4). We are grateful to Professor J. F. Fetrow, Department of Biological Sciences, SUNY at Albany, and to Mr. T. Boose for preparation of the yeast iso-1-cytochrome *c* samples. These studies were partially supported by NIH Grant GM-35103 (C.P.S.), by the Maria Skłodowska Curie U.S.–Polish Joint Fund II PAN/NIST-94-203 (A.S.), and by the Polish KBN Grant 2-PO3B-018-13 (A.S.).

REFERENCES

1. A. Sienkiewicz, K. Qu, and C. P. Scholes, Dielectric resonator-based stopped-flow EPR, *Rev. Sci. Instrum.* **65**, 68–74 (1994).
2. K. Qu, J. L. Vaughn, A. Sienkiewicz, C. P. Scholes, and J. S. Fetrow, Kinetics and motional dynamics of spin-labeled yeast iso-1-cytochrome *c*: 1. Stopped-flow EPR as a probe for protein folding/unfolding of the C-terminal helix spin-labeled at cysteine 102, *Biochemistry* **36**, 2884–2897 (1997).
3. M. Jaworski, A. Sienkiewicz, and C. P. Scholes, Double-stacked dielectric ring resonator for sensitive EPR measurements, *J. Magn. Reson.* **124**, 87–96 (1997).
4. K. M. Falkowski, C. P. Scholes, and H. Taylor, Pulse field-sweep EPR: A method of extracting hyperfine information from inhomogeneously broadened EPR lines of bioinorganic systems, *J. Magn. Reson.* **68**, 453–468 (1986).
5. C. Fan, H. Taylor, J. Bank, and C. P. Scholes, Pulse field-sweep EPR of copper proteins, *J. Magn. Reson.* **76**, 74–80 (1988).
6. J. S. Beckman, T. W. Beckman, J. Chen, P. A. Marshall, and B. A. Freeman, Apparent hydroxyl radical production by peroxyxynitrite, *Proc. Natl. Acad. Sci. USA* **87**, 1620–1624 (1990).
7. M. N. Hughes and H. G. Nicklin, The chemistry of pernitrites, *J. Chem. Soc. A* 450–452 (1968).

8. H. H. Ruf and W. Weis, Hyperfeinstruktur Des ESR-Spektrums Von Semihydro-L(+)-Ascorbinsäure, *Biochim. Biophys. Acta* **261**, 339–340 (1972).
9. W. L. Hubbell, W. Froncisz, and J. S. Hyde, Continuous and stopped-flow EPR based on a loop gap resonator, *Rev. Sci. Instrum.* **58**, 1879–1886 (1987).
10. L. Packer, Peroxynitrite, in "Methods in Enzymology," Vol. 269, pp. 285–399, Academic Press, New York (1996).
11. W. A. Pryor and G. L. Squadrito, The chemistry of peroxynitrite: A product from the reaction of nitric oxide with superoxide, *Am. J. Physiol.* **268**, L699–L722 (1995).
12. J. O. Edwards and R. C. Plumb, The chemistry of peroxynitrites, *Progr. Inorg. Chem.* **41**, 599–635 (1993).
13. D. Bartlett, D. F. Church, P. L. Bounds, and W. H. Koppenol, The kinetics of the oxidation of L-ascorbic acid by peroxynitrite, *Free Radical Biol. Med.* **18**, 85–92 (1995).
14. B. H. J. Bielski, D. A. Comstock, and R. A. Bowen, Ascorbic acid free radicals. I. Pulse radiolysis study of optical absorption and kinetic properties, *J. Am. Chem. Soc.* **93**, 5624–5629 (1971).
15. W. Colón, G. A. Elóve, L. P. Wakerm, F. Sherman, and H. Roder, Side chain packing of the N- and C-terminal helices plays a critical role in the kinetics of cytochrome *c* folding, *Biochemistry* **35**, 5538–5549 (1996).
16. T. R. Sosnick, L. Mayne, and S. W. Englander, Molecular collapse: The rate-limiting step in two-state cytochrome *c* folding, *Proteins* **24**, 413–426 (1996).